Check for updates

Remotely sensed image interpretation for assessment of land use land cover changes and settlement impact on allocated irrigation water in Multan, Pakistan

Maira Naeem · Hafiz Umar Farid · **Muhammad Arbaz Madni** ·
Rameez Ahsen · Zahid Mehmood Khan · Aqsa Dilshad · Huzaifa Shahzad

Abstract Industrial revolution and rapid population growth are responsible for alteration of land into different settlements. These changes may lead to change in land use (LU) and land cover (LC). The LULC changes have impact on hydrological regimes including streams flow pattern and allocated irrigation water (water allocation through Warabandi system). The present study aimed to identify the LULC changes and settlement impact on allocated water using the unsupervised classification and normalized difference vegetation index (NDVI) of Landsat images for the years of 1990 to 2020 in Multan District. The accuracy assessment and Kappa coefficient were also investigated to evaluate quality of results derived from the classified images. The results show that the reduction in waterbody, spare, and dense vegetation was -7.6, -1.7, and -30.7%, respectively. The settlements, barren, and crop lands have increased to 25.2, 10.1, and 4.6%, respectively, from 1990 to 2020. The values of kappa coefficient (0.84–0.85) showed very good level of classification. In addition, the volume of water loss due to change of LULC from waterbody into settlements, barren land, crop land, spare, and dense vegetation was found approximately 472, 44, 133, 54, and 85 m^3, respectively, in last 30 years. This volume of water is not reaching equitably to the farming community because of the LU and LC changes and urban settlements. The results indicated that remotely sensed image interpretation technique may be a useful for reallocation of water among farmers in an equitable and efficient way.

Keywords Remotely sensed image · LULC · Settlements · Allocated water · Accuracy assessment

M. Naeem (✉) · H. U. Farid (✉) · R. Ahsen ·
Z. M. Khan · A. Dilshad · H. Shahzad
Department of Agricultural Engineering, Bahauddin
Zakariya University, Multan 60800, Pakistan
e-mail: mairanaeem320@gmail.com

H. U. Farid
e-mail: hufarid@bzu.edu.pk

M. A. Madni
Institute of Environmental Engineering and Research
(IEER), University of Engineering and Technology
Lahore, Lahore 54890, Pakistan

Introduction

The land use land cover (LULC) change is an accelerating phenomenon on the Earth's surface driven by anthropogenic activities including urban expansion, deforestation, overexploitation of resources, or by natural processes including land sliding, flooding, soil erosion, and climatic variations (Abdulkareem et al., 2019). The change in LULC is fluctuating along areas; in rural areas, it is credited due to agriculture extension, forest fire, and illegal tree cutting, while in urban areas, it is credited to urban expansion and commercialization. LC provides the basis for interpretation of ecological potential measures and the

implementation of sustainable development (Clerici et al., 2014; Wahyunto et al., 2013; Xiuwan, 2002). The LULC has direct impacts on ecosystems and their associated services, particularly on water allocation. Water allocation is the phenomenon of supply of water to meet requirements of a community. The LU and LC changes are important to hydrological study as it has great influence on sediment yield, surface water runoff, and nutrient load from agricultural practices. In recent years, change in LC is to be considered as a factor of environmental change throughout the world (Ahmad, 2013; Quyen et al., 2014; Udin & Zahuri, 2017). Land use (LU) is referred as reason for recreation, wildlife habitat, or agriculture which includes controlling and converting the natural world into a man-made environment. LC relates to ground surface cover such as trees, urban infrastructure, water, and bare soil (Rujoiu-Mare & Mihai, 2016). The LC identification is baseline information for thematic mapping and change detection analysis. The LULC change detection becomes central component in planning, monitoring, and managing natural resources for sustainable development (Milad et al., 2015).

Climate change has evolved into a challenging process worldwide that has enhanced the level of uncertainty in the atmosphere. Furthermore, growing urbanization leads to significant changes in LULC patterns all over the world, amplifying the detrimental effects of climate change and the hydrologic ecosystem (Liang et al., 2021; Wang et al., 2014). Rural to urban conversion is happening at an unprecedented rate in recent human history, and it is having a huge impact on ecosystems, biodiversity, and the environment (Ullah et al., 2019; Zhou & Chen, 2018). The world's total urban area raised by 168% between 2001 and 2018, with Africa and Asia experiencing the most rapid growth (Dewan et al., 2021). In 2018, 55% of the world's population lived in cities, a figure that is expected to raise 68% by 2050. Asia and Africa have accounted for almost 90% of urban population growth (Ranagalage et al., 2021). Humans have altered around half of the land surface, and anthropogenic land use is projected to expand in the future to meet rising land demand (Brovkin et al., 2013; Yohannes et al., 2021). Human beings are experiencing multiple hazards from natural and artificial disasters because of global environmental change and rapid economic and social expansion (Huq et al., n.d.). Land use

changes and climatic variability are thought to be linked to natural disasters. Flooding is anticipated to become more common because of anthropogenic climate change. Several studies have found that changes in LC are linked to an increase in flooding areas (Adnan et al., 2020; Dewan & Yamaguchi, 2009; Roy et al., 2020).

Floods were responsible for 47% of natural disasters between 1995 and 2015 in Southeast Asia (Rahman et al., 2021). Climate change is one of the world's most pressing issues today, particularly because of its numerous and unpredictable effects on water resources. Since the industrial revolution, anthropogenic warming has led glaciers to recede all around the planet (Hayat et al., 2019). Rapid urbanization resulted in LULC changes, which increased the temperature of the land surface. Crop yields are significantly impacted by temperature fluctuations and uncertainty in rainfall patterns (Gul et al., 2020; Mashwani, 2020). Moreover, these LULC changes contributed about one-third of all anthropogenic carbon emissions since the industrial revolution (Iqra et al., 2020; Zhao et al., 2021). Agriculture and food security are both being impacted by climate change. According to the most recent United Nations (UN) population predictions (medium variation), the world's population would expand from 7 billion in 2010 to 9.8 billion in 2050. Moreover, UN predicted that more than 70% of the world's urban population will be increased by 2050 (Hussain et al., 2020) (Comission, 2018).

Remote sensing (RS) has been the core means of land management because it includes the acquisition of spatial information with high update speed for the benefits of economic convenience and fast spatial information (Setiawan et al., 2014; Anchan et al., 2018). Geographic information system and remote sensing are the most efficient methods for identification and detection of land use patterns for geo-referencing, digital formatting and spatial data acquisition (Chen et al., 2005; Lu et al., 2004; Nuñez et al., 2008; Rahman et al., 2012).

Satellite imagery data is usually used for LU and LC analysis through aerial photographs. More accurate method for the study of LC change have been developed with advancement of remote sensing techniques and open access to satellite data which includes LANDSAT (Land Remote Sensing Satellite System), spaceborne high-resolution sensors, and MODIS (Moderate Resolution Imaging Spectral

Radiometer) for research (Goldblatt et al., 2018; Patela et al., 2015). The remote sensing application has potential for land cover monitoring at high resolution through spectral response. Satellite imagery is valuable because of its rich spatial information and repetitive coverage. Digital data processing is very useful because accurate LU and LC classes can be computed using normalized difference vegetation index (NDVI) techniques (Butt et al., 2015; Khatami et al., 2016). The GIS and RS provide an easy, accurate, cost-effective, and a time-saving alternative to understanding landscape dynamics (Kalra et al., 2013). The image classification method involves the conversion of multiple raster band images into a single raster band image with definite classes associated with different land covers. Typically, image classification is a dynamic process with various land use features in assessment of land cover (Araya & Hergarten, 2008; Kalra et al., 2013). The application of the RS in classification deals with the clustering of image's pixels into number of classes in such a way that pixels have identical properties is merged in the same class. In unsupervised classification, grouping of pixels is based on unlabeled data. The unsupervised classification is used to map the radioelement classes which is used in discrete statistical operations (Ahmad et al., 1992; Araya & Hergarten, 2008; Lu & Weng, 2007).

NDVI is performed in unsupervised classification to determine the directories such as forest cover, spare vegetation, dense vegetation, barren land, urban land, and water bodies (Meneses-Tovar, 2011; Vicente-Serrano et al., 2016). The temporal variation relates growth and change in vegetation which exhibit areas that have the same vegetation. The categorization of the NDVI information resulting from satellite images is subsidized to time lapse of remote sensing data which plays vital role in LC classification (Chen et al., 2015; DeFries et al., 1995; Tian et al., 2015). Urban expansion, rapid population growth, and industrial revolution are responsible for conversion of rich lands into human settlements and led to several challenges for irrigation water allocation. Water allocation is the process in which an available water resource is distributed to legal applicants. A rotating water allocation system that is practiced in Pakistan is Warabandi that shares irrigation water equally and efficiently. Due to the conversion of irrigated land into urban settlements and other land use, there is a need to assess the volume of allocated irrigation water for

that area. The assessment allocated irrigation water for urban settlements and other LU may help to reallocate it among the farmers in equitable way. Therefore, present study was conducted to delineate the various LULC classes in Multan District for the years 1990 and 2020 and to quantify the land consumption rate and changes in LULC classes. The identification of vegetation changes in the Multan District due to urban expansion in the recent decades and influence of different settlements on allocated water has also been investigated using satellite images interpretation in Multan (Pakistan).

Materials and methods

Study area

The present study was conducted in Multan District, Pakistan, as shown in Fig. 1. The study area lies at 30°11′52″ N and 71°28′11″ E. Its average elevation is 122 m (Ahsen et al., 2020). The Multan District consists of four tehsils: Multan City, Multan Saddar, Jalalpur Pirwala, and Shujaabad. Multan District is delineated by Chenab River on its western side. The main canal for irrigation water supply in Multan District is Sidhnai canal with gross command area of 0.349 million ha. The minimum and maximum temperatures of the study area in summer are 26 °C and 50 °C, respectively. In winter, the minimum temperature is 4.8 °C and maximum temperature is 23.4 °C. The average annual temperature of district Multan is 25.6 °C. Multan District is in arid region, and it receives about 200 mm of rainfall per year. There are two main growing seasons in district Multan i-e Rabbi and Kharif. Cotton is the major crop of Kharif season. It is sown in April–May and is harvest in October–December. Wheat is the major crop of Rabbi season. Wheat is sown in October–December and harvested in April–May (Hussain et al., 2020).

Satellite data acquisition

NASA GLCF (Global Land Cover Facility) provides the latest high-resolution satellite images without any charge. It has developed a chance for monitoring land cover anywhere on earth using the remote sensing technique in a cost effective manner (Chemura et al., 2020). The satellite images of Landsat were utilized for the years 1990
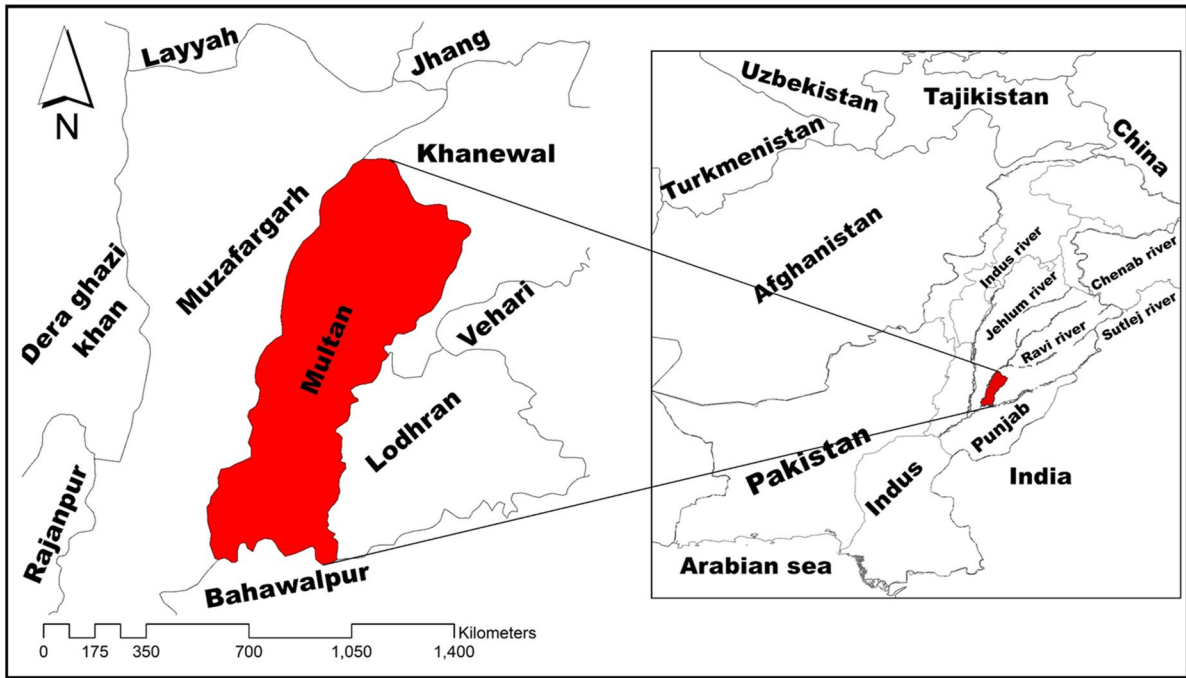
Fig. 1 Location of the study area

and 2020 for visual inspection, LU, and LC classification. The Landsat images having 30-m spatial resolution and 16-day temporal resolution were obtained from Earth Explorer (http://earthexplorer.usgs.gov/) website (Rawat, 2015). The characteristics of Landsat images are given in Table 1. For classification purpose, unwanted shade and cloud free image was selected because image having cloud can decrease accuracy. The image was inspected with the different identifiable objects on the ground surface. Spectral information was used to relate ground features.

Digital image processing

Landsat images were operated by the software-assisted interpretation. The study made the use of image processing software's ArcMap 10.7.1 and ERDAS IMAGINE 9.1, to achieve the objectives. Pre-processing of images using ERDAS IMAGINE includes the geo-referencing, composite image processing, mosaicking, and sub-setting (Fig. 2). The accurate base map of the study area is taken from survey of Pakistan in order to make the land use land cover classification (Rawat, 2015). The shape file was created to create digitized polygons in ArcGIS 10.7.1. The global positioning system (GPS) points of

imagery data were imported in ArcMap to execute identification of land cover. By using topographic map of the study area, data was projected to a UTM coordinate system having Datum WGS 1984.

Table 1 Description of remote sensing data used in spatial analysis

Description	1990	2020
Acquisition date	26 May	28 May
Satellite	Landsat 5	Landsat 8
Sensor type	TM	OLI_TIRS
Geo-referencing	150/39 150/40	150/39 150/40
Resolution	30 m	30 m
Cloud cover	0.00	3.33
Projection	UTM43N	UTM43N
Sun azimuth	100.6902115	109.3074943
Sun elevation	60.40119001	68.78002522
Spectral bands	B1 Blue: 0.45–0.52 B2 Green: 0.52–0.60 B3 Red: 0.63–0.69 B4 NIR: 0.77–0.90	B2 Blue: 0.45–0.51 B3 Green: 0.53–0.59 B4 Red: 0.64–0.67 B5 NIR: 0.85–0.88

Fig. 2 Flow chart summarizing the method of the LULC change detection and water allocation
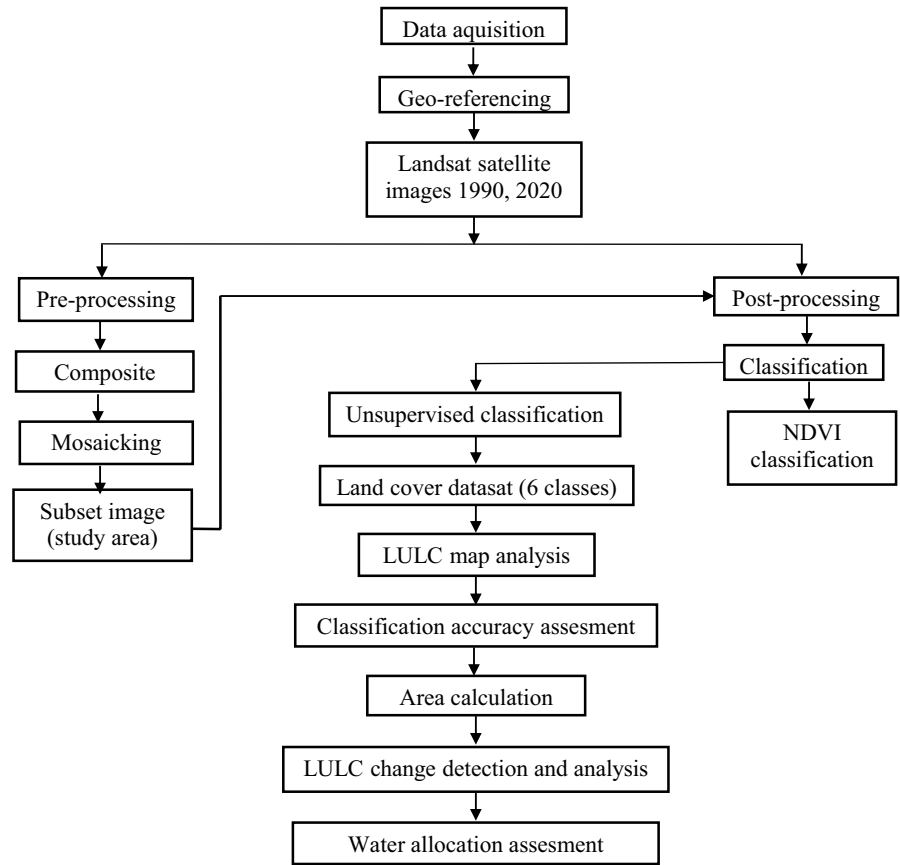
Normalized difference vegetation index analysis

Vegetative indexes describe the soil and vegetation cover distribution which rely on the reflection patterns of different vegetations. Normalized difference vegetation index (NDVI) analysis is considered as most accurate method for digital image processing (Allawai & Ahmed, 2020). In this study, NDVI method was used for identifying various land use features from satellite images of Multan District. For betterment results, NDVI was used to classify the Landsat data of 1990 and 2020. The NDVI was calculated as per-pixel values based on red and near infrared bands of images (Eq. 1).

$$NDVI = \frac{(NIR - RED)}{(NIR + RED)} \tag{1}$$

where RED is visible red reflectance with range of (600–700 nm), and NIR is near infrared reflectance with range of (750–1300 nm). The wavelength range and characteristics of images are given in Table 1. NDVI values were ranged from −1 to +1. The values closer to +1 were correlated to denser green vegetation, and 0 values were correlated to least or no vegetation. The negative values were used to represent water bodies (Zaidi et al., 2017). The classification of features and range of the NDVI values are given in Table 2.

Image classification

The unsupervised classification was used in this study according to NDVI values. The defined classes were waterbody, settlements, barren land, crop land, spare, and dense vegetations (Table 3). In Fig. 3, blue color shows waterbodies, red color shows settlements, orange color shows barren land, light green color shows crop land, moderate green color shows spare vegetation, and dark green color shows dense vegetation. For unsupervised classification, ERDAS Imagine was used to engages the Iterative Self-Organizing Data Analysis Technique Algorithm (ISODATA) clustering scheme which is used to group the pixels with similar features based upon

Table 2 NDVI classified values for different land covers

Class	Land feature	Avg. values
1	Water bodies	−0.96–0.015
2	Settlements	0.015–0.14
3	Barren land	0.14–0.18
4	Crop land	0.18–0.27
5	Spare vegetation	0.27–0.36
6	Dense vegetation	0.36–0.94

software without any sample classes. (Anwar Khalid, 2019). By allotting per-pixel signatures to differentiate the area into six classes which is based on the Digital Number value of landscape features.

Accuracy valuation

After classification of land features, it is important to assess the standard of information derived from satellite image. In this study, accuracy was calculated using the error matrices grounded on a class-conscious random sampling method, in which 15 minimum reference points from every class were taken. For visual interpretation of accuracy assessment 90 ground truth points were taken from Google Earth Pro. Reference data were compared with the classification results. The accuracy of every class was estimated using the overall accuracy (OA), user accuracy (UA), and producer accuracy (PA). One of the renowned methods for accuracy assessment is kappa coefficient (K) which measures the degree of accuracy for classification. The value of kappa lies between 0 and 1, where 0 signifies the chance of class existence and 1 signifies perfect agreement between both data sets. Kappa in Eq. (2) is typically expressed as

$$k = \frac{N^* \sum_{i=1}^{k} x_{ii} - \sum_{i=1}^{k} (x_{i+} * x_{+i})}{N^2 - \sum_{i=1}^{k} (x_{i+} * x_{+i})} \quad (2)$$

where N is the total samples, x_{ii} is the corrected samples (diagonal), x_{i+} is the marginal row total, and x_{+i} is the marginal column total. The values which are higher than 0.85 signify excellent agreement, values from 0.85 to 0.7 signify very good agreement, values from 0.7 to 0.55 signify good agreement, values from 0.55 to 0.4 signify fair agreement, and values lower than 0.4 signify very poor agreement between images (Monserud & Leemans, 1992).

Land use/cover change detection and analysis

Change detection defines the differences between satellite images of the same scene at different time intervals. Inspecting the Earth from space is key to the understand the influence of anthropogenic activities and natural resource utilization with the passage of time (Ganasri & Dwarakish, 2015; Rawat et al., 2013). The classification of land use features provides all the necessary information regarding utilization of landscape. Post-classification detection technique was performed in ERDAS imagine. A pixel-based evaluation was done to obtain information (Mohammed et al., 2018). Areal data of two different times were computed using cross tabulation to investigate qualitative and quantitative aspects of land use changes from 1990 to 2020. A change matrix is created from this method with the help of ERDAS imagine.

Water allocation assessment

The water allocation has been identified as a priority water management issue because of the growing demand for water, especially from the rural sector. The farmers need reasonable amount of water to meet the irrigation requirement (Li et al., 2020). The warabandi system has been adopted in most of the regions
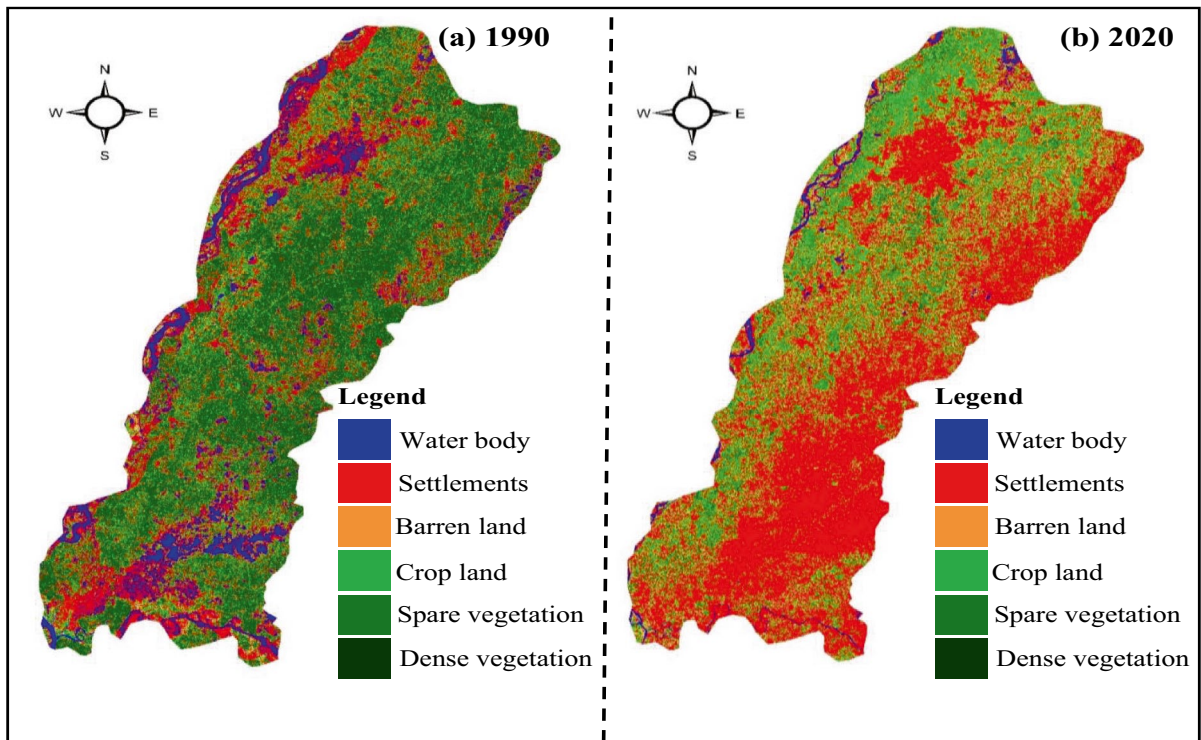
Table 3 Classes delineated based on unsupervised classification

Sr no	Class term	Explanation
1	Waterbodies	Open water bodies, river, perennial canals, and reservoirs
2	Settlements	The class includes different settlements, residential, industrial, commercial roads, villages, and artificial infrastructure
3	Barren land	Land areas with exposed soil surface and land capable of producing no vegetation
4	Crop land	Open areas with crops and grasses
5	Spare vegetation	Sparse trees of lower denseness that cannot be deliberated as forests
6	Dense vegetation	An area covered with mature trees and other plants growing in large area

Fig. 3 Classified maps of District Multan for **a** 1990 and **b** 2020

particularly in the district Multan for the farmers to meet their crop water requirement. The land use land cover has been changing at a phenomenal growth rate due to urbanization and development of major industries. Due to land cover change, water bodies have also been changing at rapid rates which create the water allocation problems (Algorithms et al., 2007). In present study, it was estimated that how much water body is converted to other land use categories and how much volume of water is changed from 1990 to 2020.

Results

The land use (LU) and land cover (LC) maps of Multan District for 1990 and 2020 were obtained by multi-temporal quantification of satellite imageries (Fig. 3). Figure 4 depicts LU and LC distribution in different land use categories. Figures 5 and 6 illustrate magnitude of change in different land categories. Figure 7 describes the change in LC for 30 years' period in each land use category. A brief description of these results is given in subsequent section.

Land use/land cover status

Figure 3 shows the classified maps of the Multan District for 1990 and 2020. Figure 3a shows that in 1990, the study area had greater contribution to water body, spare vegetation, and dense vegetation. In contrast, settlements, barren land, and crop land had less contribution in the study area. Figure 3b shows that in 2020, most of the area had changed into settlements, barren land, and crop land. Likewise, the water body, spare vegetation, and dense vegetation had decreased to a considerable amount. It is clear from Fig. 3 that a spot shown in northwest side of study area has greater contribution to water body in 1990. In 2020, it had converted to settlements. Numerical results of area and amount of change in different LU and LC categories in Multan District during 1990–2020 are displayed in Table 4. In 1990, about 8.9% (or 36,150 ha) area of Multan District was under waterbody, 26.2% (or 106,035 ha) was under settlements, 2.6% (or 10,503 ha) was under barren land, 15.5% (or 62,843 ha) was under crop land, 13.4% (or 54,092 ha) area was covered by spare vegetation, and
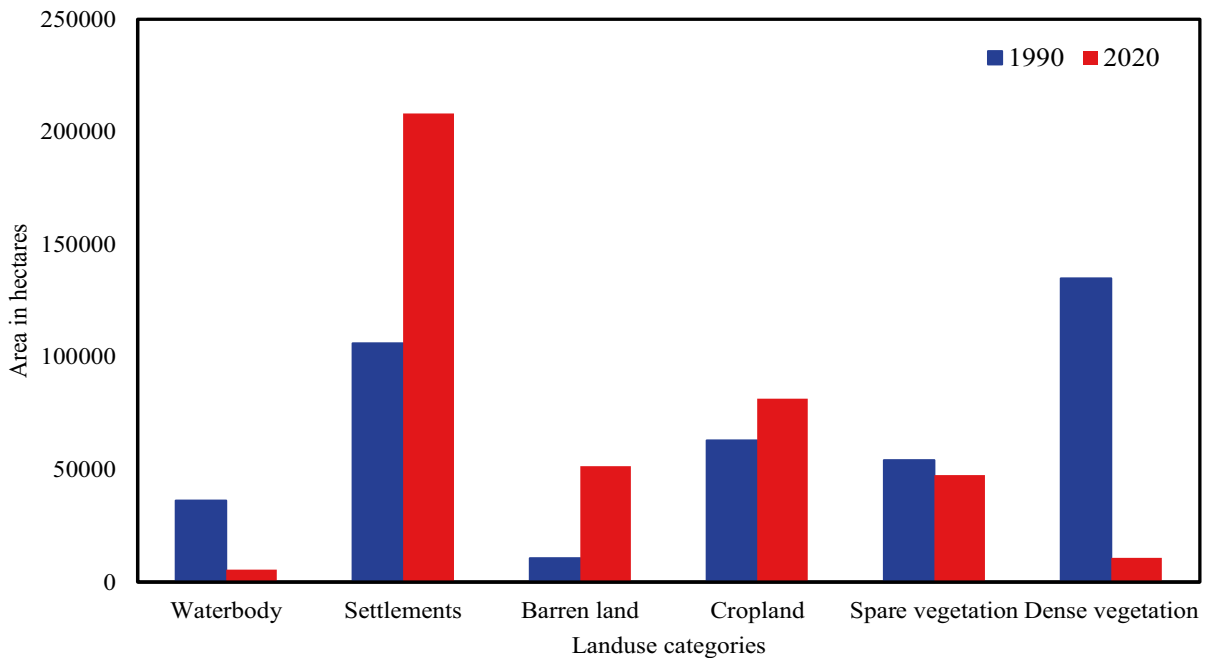
Fig. 4 Land use distribution of District Multan in 1990 and 2020

33.3% (or 134,863 ha) was under dense vegetation. During 2020, the area under these land use categories was found as 1.4% (or 5519 ha) under waterbody, 51.5% (or 208,141 ha) under settlements, 12.7% (or 51,441 ha) under barren land, 20.1% (or 81,341 ha) under cropland, 11.7% (or 47,417 ha) under spare vegetation, and 2.6% (or 10,629 ha) under dense vegetation.

Classification accuracy assessment

To evaluate the quality of information derived from classified images of 1990 and 2020, the accuracy assessment was carried out. Accuracy assessment was performed for each LU and LC map by comparing the random samples with reference points using the Google Earth. The accuracy assessment for classified images was carried out by taking ninety (90) ground truth points, considering fifteen (15) from each class. Table 5 represents the accuracy assessment (user and producer accuracy) of classification for 1990 and 2020. In addition, the overall accuracy achieved for classified images of 1990 and 2020 was 87.77% and 86.66%, respectively. Separation was found good between settlement and vegetation classes. Another method used for the evaluation of results is kappa coefficient. The values of Kappa coefficient for 1990 were 0.85 and 0.84 for 2020. Kappa value for this study shows very good level of classification as represented in Table 6.

Change detection analysis

The data presented in Table 4 and Fig. 3 depict that positive and negative changes occurred in LC pattern of the study area. The dominant factors of the land degradation were identified in the study area. It was observed that the main type of human-induced land degradation in the inspected areas is urbanization. During the last three decades, the settlements have increased from 26.2% in 1990 to 51.5% in 2020 due to the increasing rates of built-up land. This showed that 25.2% of the total area has changed to settlements. On the other hand, the dense vegetation has decreased from 33.3% in 1990 to 2.6% in 2020 because of the urban growth. This change accounts for 30.7% of the total area of Multan District (Fig. 4). Similarly, the spare vegetation has slightly decreased from 13.4% in 1990 to 11.7% in 2020 which accounts for 1.7% of the total area.
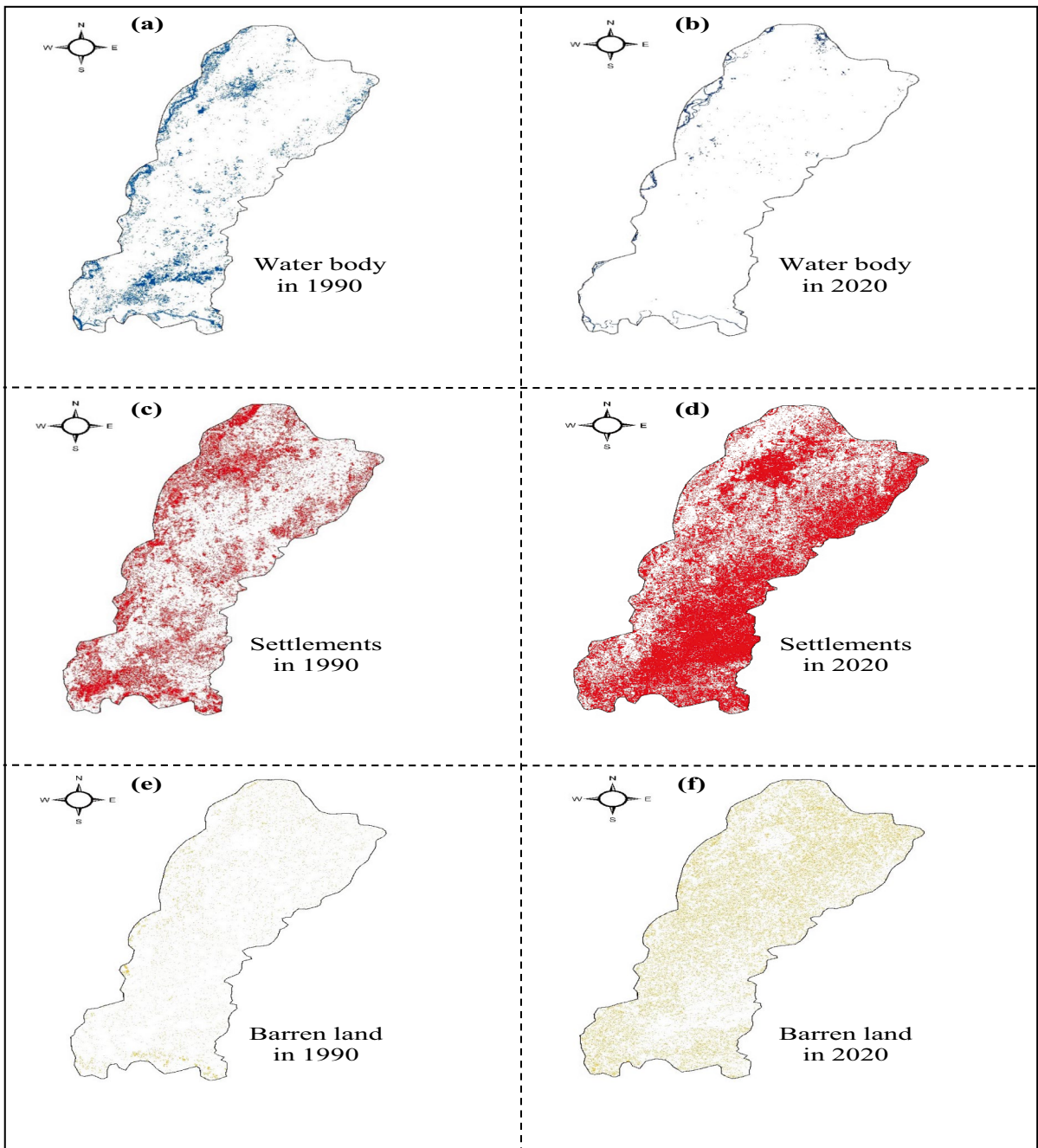
Fig. 5 Land cover status of District Multan: **a** waterbody in 1990, **b** waterbody in 2020, **c** settlements in 1990, **d** settlements in 2020, **e** barren land in 1990, and **f** Barren land in 2020

The water body has also decreased from 8.9% in 1990 to 1.4% in 2020. The decline in water bodies from last three decades is due to either urban infrastructure or rapid population growth which directly affects the land cover of the area. From the identified land use categories, the highest category was dense vegetation in 1990 while in 2020 settlements become the highest one (Table 4).

Fig. 6 Land cover status of District Multan: **a** crop land in 1990, **b** crop land in 2020, **c** spare vegetation in 1990, **d** Spare vegetation in 2020, **e** dense vegetation in 1990, and **f** dense vegetation in 2020
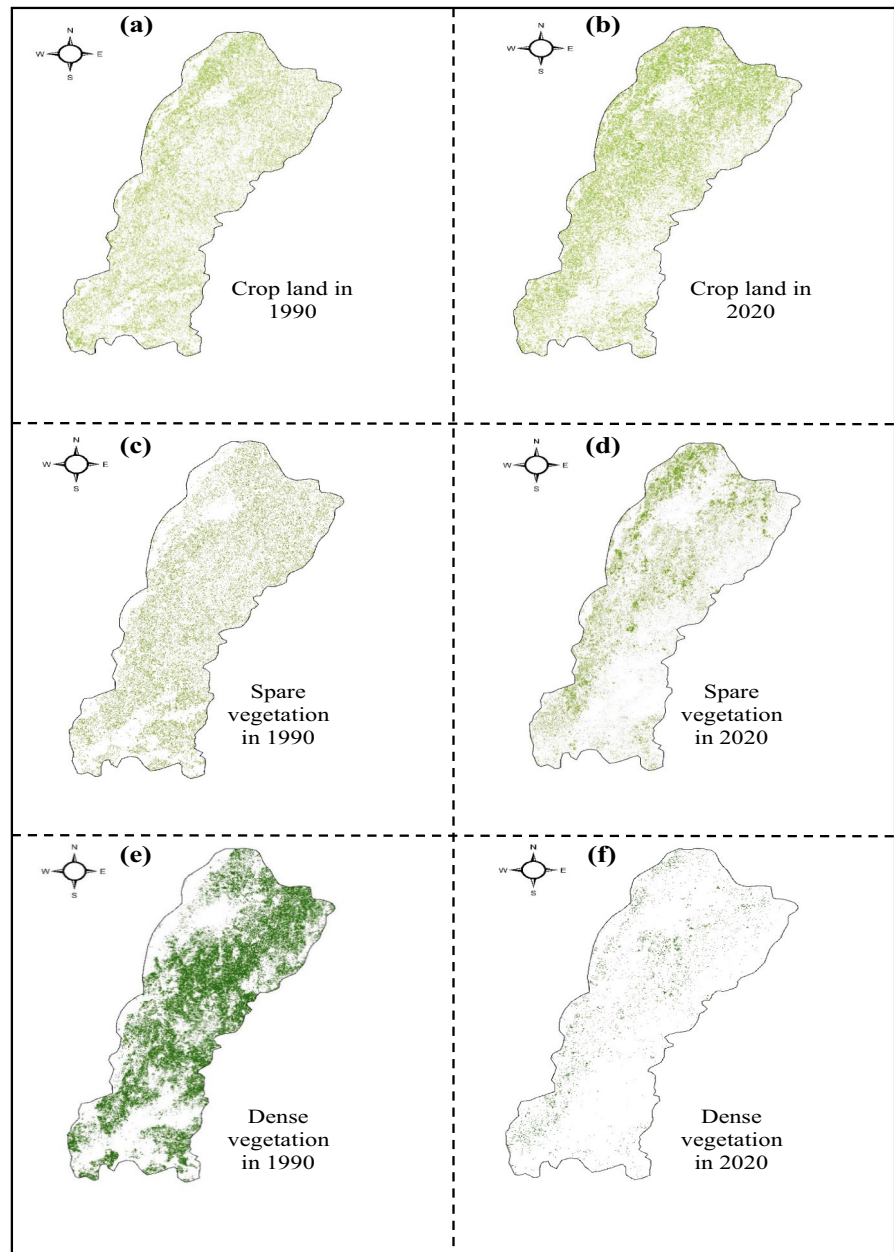
Reclassification of the results is performed to analyze the location of areas which are changing rapidly in the given time frame (Fig. 5a–f). Figure 5a shows the areas having waterbody and its pattern in 1990, while Fig. 5b shows waterbody for 2020. In 1990, the NW and SE side of the Multan District showed considerable amount of water bodies. In 2020, not only waterbodies get depleted but also the settlements

become much more in the same areas. It can be seen from Fig. 5a, b that barren land has increased in the given time frame. The reason is that the vegetation is continuously decreasing so these classes become barren and then slowly converted to settlements. Similarly, Fig. 6a–f represent that crop land is increasing with a slow rate, but the spare vegetation and dense vegetation is decreasing with rapid rates.
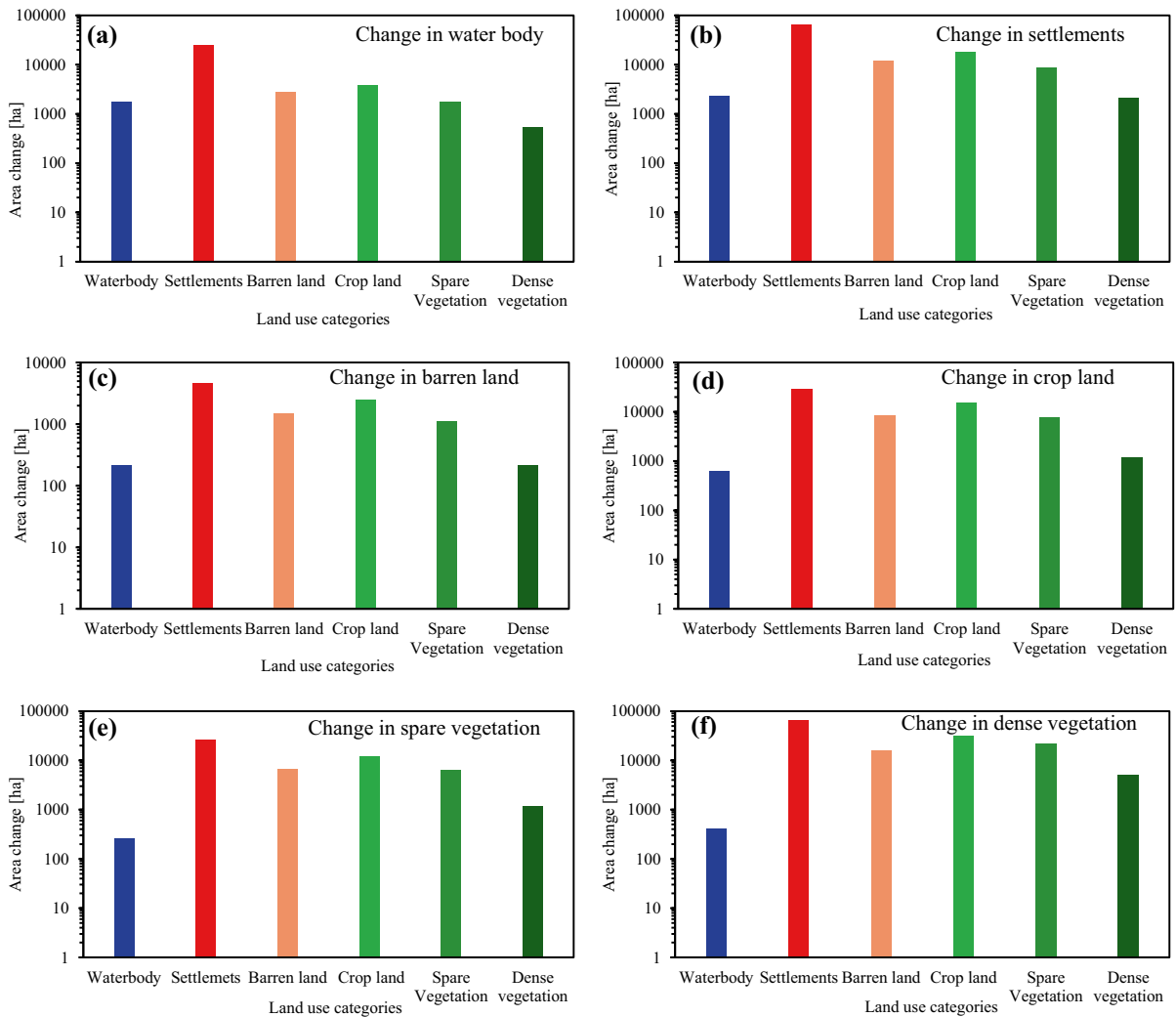
Fig. 7 Land use land cover change in District Multan for **a** water body, **b** settlements, **c** barren land, **d** cropland, **e** spare vegetation, and **f** dense vegetation

Table 4 Results of area and amount of change in different land use/cover categories in District Multan during 1990–2020

Land use/cover categories	1990		2020		Change 1990–2020	
	Area (ha)	% Area	Area (ha)	% area	Area (ha)	% change
Waterbody	36,150	8.9	5519	1.4	−30,632	−7.6
Settlements	106,035	26.2	208,141	51.5	102,106	25.2
Barren land	10,503	2.6	51,441	12.7	40,938	10.1
Crop land	62,843	15.5	81,341	20.1	18,498	4.6
Spare vegetation	54,092	13.4	47,417	11.7	−6675	−1.7
Dense vegetation	134,863	33.3	10,629	2.6	−124,234	−30.7
Total	404,487	100.0	404,487	100.0		

Table 5 Accuracy assessment of the land use land cover categories

LULC classes	User's accuracy		Producer's accuracy	
	1990	2020	1990	2020
Waterbody	100.0	93.3	100.0	87.5
Built-up land	93.3	86.7	82.4	76.5
Barren land	73.3	73.3	84.6	91.7
Shrub/grassland	80.0	86.7	85.7	81.3
Spare vegetation	86.7	80.0	81.3	92.3
Dense vegetation	93.3	100.0	93.3	93.8

Table 6 Accuracy evaluation using Kappa coefficient statistics

Year	Overall accuracy	Kappa coefficient
1990	87.77	0.85
2020	86.66	0.84

Transitional probability matrix

Change detection matrix was prepared to understand the land utilization of different LC classes in past three decades. Table 7 shows cross tabulation of land cover categories based on time frame data of 1990 to 2020. The 5475-ha area was waterbody in 1990, and about 31.2% (1708 ha) were waterbody in 2020. These results showed that 41.2% area has converted to settlements. The remaining 3.8% (210 ha) and 23.8% (2257 ha) have converted to barren lands and different vegetation classes, respectively. In 1990, the area of barren land was 47,667 ha, out of which

about 3.1% (1504 ha) were also barren lands in 2020. The 5.7, 25.3, and 65.9% area of the barren land have converted to waterbody, settlements, and different vegetation classes, respectively. About 10,277 ha was covered by dense vegetation in 1990 and 5106 ha (49.6%) was covered by dense vegetation in 2020. These results showed that 50.4% area that was covered by dense vegetation in 1990 has converted to other LC classes in 2020, i.e., 5.1% (531 ha) has converted to waterbody, 20% (2062 ha) has converted to settlements, and the rest of 25.3% has converted to different vegetation classes. Figure 7a–f show the LULC in Multan District for each category. Figure 8 shows graphical illustration of percentage (%) change in LULC categories for Multan District from 1990 to 2020. The reduction in waterbody, spare vegetation, and dense vegetation were found about $-7.6, -1.7,$ and -30.7%, respectively. In contrast, the increase in settlements, barren land, and crop land were found 25.2%, 10.3%, and 4.6%, respectively.

Water allocation assessment

Table 8 shows volume of water change due to change in different LU and LC categories in Multan District from 1990 to 2020. The loss in volume of water (472 m^3) due to conversion of waterbody to settlements was observed. Similarly, 44, 54, 133, and 85 m^3 loss in volume of water for barren land, spare vegetation crop land and dense vegetation were found, respectively. However, total volume of water loss in Multan District due to LULC change during the last three decades was 788 m^3. This volume of water is not reaching equitably to the farming community because of the LU and LC changes. The results indicated that due to the urban settlements, there is a strong need of reallocation water among farmers in equitable way.

Table 7 Transitional probability matrix of land cover categories based on time frame data 1990–2020 (hectare)

		1990						
		Waterbody	Settlements	Barren land	Crop land	Spare vegetation	Dense vegetation	Total
2020	Waterbody	1708	2463	2723	3748	1758	531	11,224
	Settlements	2257	87,509	12,098	17,677	8686	2063	42,781
	Barren land	211	4620	1505	2433	1095	214	8573
	Crop land	635	28,561	8588	15,217	7750	1191	46,725
	Spare vegetation	256	25,337	6749	12,188	6344	1172	45,702
	Dense vegetation	408	63,165	16,004	30,882	21,468	5107	131,927
	Total change	5475	211,654	47,668	82,145	47,100	10,278	286,930

Fig. 8 Percentage (%) change in land use/cover categories for District Multan (1990 and 2020)
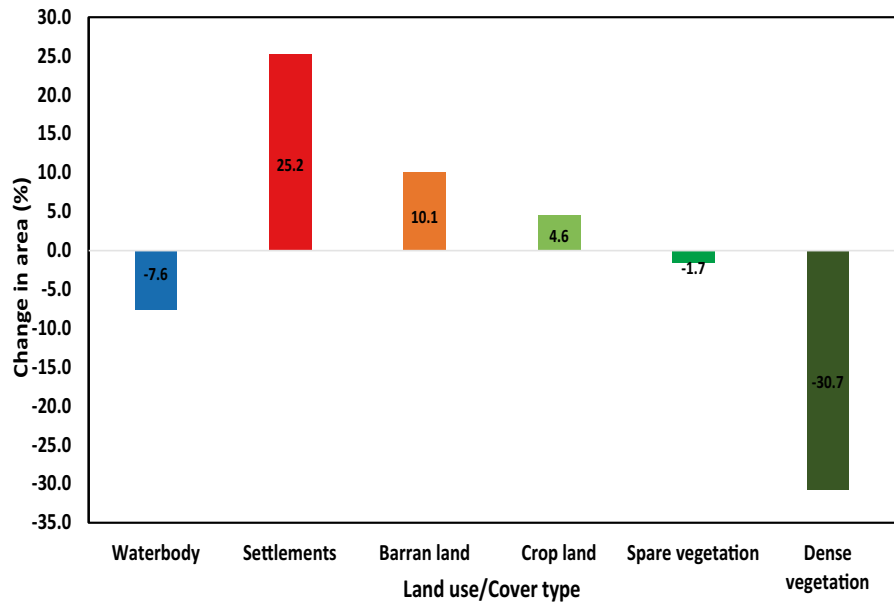
Discussion

The satellite imagery datasets are in raw form and cannot be directly used to produce LULC maps. So, these datasets were primarily processed in ERDAS Imagine and NDVI maps were created to distinguish among various classes. The classified images of 1990 and 2020 show spatial and temporal distribution of LULC classes of Multan District. Due to urban expansion and industrialization, the LULC change becomes an accelerating phenomenon worldwide which is responsible for the conversion of green lands such as forests and spare vegetation into human settlements and agricultural lands. Quantitative and qualitative assessments of LULC changes are necessary to predict the impacts of these changes in natural vegetation pattern on the Earth's surface.

Table 8 Volume of water change from 1990 to 2020 due to change in different LULC categories in Multan District

Land use category	Area (Ha)	Volume of water (m^3)
Settlements	2257	472
Barren land	211	44
Crop land	635	133
Spare vegetation	256	54
Dense vegetation	408	85
Total	3767	788

Multan's dense vegetation has been impacted by urbanization since it has degraded swiftly and been transformed to diverse land uses. In this study, satellite imageries are utilized to detect the amount of land use changes in Multan District using a simple and inexpensive technique based on remote sensing and GIS. The trend of land use changes, expressed as a percentage increase in deforested area and a reduction in natural vegetation cover, will aid policy makers in making appropriate decisions to improve the situation and conserve natural habitat and wildlife. The dominant land cover feature of Multan District was dense vegetation in 1990. However, within 30 years, it has decreased by more than 70%. The transition matrix reveals that settlements were typically formed from dense vegetation. Alternatively, settlements have increased by more than 50% in the last three decades. Unsupervised land use classification was found to be a preferable option for land use research and multi-temporal change evaluation in this study. The overall classification accuracy and the kappa value for 1990 and 2020 and unsupervised land use classification were sufficient to detect Multan's changing scenarios.

According to Butt et al. (2015), Simly watershed in Islamabad shows the decrease in Vegetation cover and water classes, whereas the settlements, bare land, and agriculture land were increased. Vegetation cover declines from 69% in 1992 to 43% in 2012, while the least area covering class was waterbody in 1992,

which further lost area from 4 to 1%. The settlements increased from 6 up to 11% of the total area. The agriculture land was increased from 11 to 29%. The major impact of settlements and agriculture land was subjected on dense vegetation and waterbody to deforestation and water depletion, respectively (Butt et al., 2015). Due to land cover change, water bodies has also been changing at rapid rates which create the water allocation problems (Algorithms et al., 2007). Due to LULC change, there are uncertainties of fluctuating water supply. Therefore, proper planning for the use of agricultural water resources is necessary (Algorithms et al., 2007). The studies identified optimum planting date and change in allocation of agricultural irrigation water to improve irrigation water use efficiency using the crop growth models (Rahman et al., 2019; Mubeen et al., 2020; Fahad & Wajid, 2020). Another study of Hassan et al. (2016) on LULC change in Islamabad Pakistan showed a positive change of 213% in urban area from 1992 to 2012. The results show that Barren area had the largest share of 55.35% in 1992 and it was reduced to 1.87% in 2012. The forest area also decreased from 13.49 to 6.82% during the study period. The major increment was faced by built-up land which accounts 18.09% in 1992 to 56.73% in 2012. The study also showed the increase in agricultural area from 11.49 to 32.23% from 1992 to 2012. These values indicated the dramatic LULC change because of conversion of barren land and forest to urban areas which caused diverse and extensive environmental degradation in Islamabad (Hassan et al., 2016).

The major factors observed behind the LULC changes in the study area is loss of valuable land resources, water deficiency, population growth, agricultural expansion, urban area expansion, and economic development (Sahebjalal & Dashtekian, 2013). In addition to human factors, climate change has significant impact on LULC changes. Rapid urbanization resulted in LULC changes, which increased the temperature of the land surface as the built-up land have high land surface temperature (LST) as compared to vegetation land (Hussain et al., 2020). Land use change in terms of installing brick kiln industries, transforming of wetland into urban land, exchange of land between mango orchard and agricultural land, etc., are some vital causes behind surface temperature change in the urban fringe area. Considering this trend, immediate land transformation policies should

be reviewed specially regarding transforming mango orchard and wetland. (Pal & Ziaul, 2017). Deforestation and habitat loss were the major impacts of urbanization on the environment. The irrational way of land use such as conversion from woodland to farmland has led to land degradation, however through reallocation of land that has been excessively exploited to a new use (Choudhary et al., 2015).

Rawat et al. (2013) conducted a study in Uttarakhand, India; the results show that fluctuations occurred in the LULC pattern during the last two decades (1990–2010). The built-up land has increased from 1.25 to 4.08 km^2 which accounts for 8.88% of the total study area. Similarly, vegetation cover has decreased from 10.29 to 7.29 km^2 which accounts 9.41% of total area. The NDVI is implemented in Image classification for better accuracies (Rawat et al., 2013). The LULC change detection results for the Harangi catchment region in Karnataka State, India, showed a significant change in forest area, plantation, and waste land between 2007 and 2013. The forest area declined substantially from 183.12 to 131.02 km^2. The amount of waste land has been reduced from 72.85 to 57.14 km^2. Fallow land and water bodies have also been reduced from 68.89 to 42.63 km^2 and 6.71 to 3.82 km^2, respectively. Alternatively, the urban area has been increased from 13.06 to 13.72 km^2. Because of improved living style of the population in this region, the results displayed an increase in urban area and plantation from 2007 to 2013. Agriculture is the predominant occupation in the study area because it is a rural catchment. As a result, the amount of forest and waste land has substantially reduced (Ganasri & Dwarakish, 2015).

Milad et al. (2015) conducted a study to measure the LC change in Seremban, Malaysia, using NDVI index. The results showed that substantial changes in Seremban, Malaysia, confirmed the expansion of the non-vegetation class from 3390 ha in 1990 to 6914 ha in 2010. However, due to urbanization and oil palm plantings in dense forest areas, the class of dense vegetation cover declined from 74,934 ha in 1990 to 62,412 ha in 2010. Furthermore, rapid population increase is a serious concern that has a significant impact on the city of Seremban's LC and utilization (Milad et al., 2015). Rujoiu-Mare et al. (2016) present a method for obtaining the LC dataset for a specific Subcarpathian area in Romania's Prahova County. In this study, the link between the ground truth points

and the LC dataset was compared using a confusion matrix approach. Based on errors of omission and commission on the non-diagonal lines of the error matrix, this method reflects the agreement between the current LC raster and the ground truth using four accuracy measures: the producer's accuracy, the user's accuracy, the overall accuracy, and the kappa coefficient (rows and columns). The higher accuracy of the final LC dataset shows the utility of this method (Rujoiu-Mare & Mihai, 2016).

Islam et al. (2018) used multi-temporal remotely sensed imagery to investigate LU classification and change detection, Chunati wildlife sanctuary, Bangladesh. The study's findings on LU changes, specifically the percentage rise in deforested land and decrease in natural vegetation cover, may enable policymakers in making appropriate steps to reverse the situation and conserve natural habitat and species (Islam et al., 2018). Adding socioeconomic and demographic data from the research region, as well as temporal change patterns, would provide crucial reasoning for LULC assessment. As a result, the findings of this study demonstrate that change detection techniques like as NDVI and unsupervised classification utilizing LANDSAT data can be used to characterize and comprehend LULC changes in transitional areas such as Multan, Pakistan.

Conclusions

Land use (LU) and land cover (LC) have changed significantly in recent decades because of rapid population growth, industrialization, and commercialization. Being an agriculture dependent country, these changes have a momentous impact on allocated irrigation water. Multi temporal satellite imagery and remote sensing together with GIS techniques play a vital role to monitor urban development over time by creating accurate LU and LC changes maps. In this regard, the present study identifies LU and LC changes impact on allocated irrigation water using unsupervised and NDVI classification of satellite images for the years 1990 and 2020 in Multan District. The LU and LC change assessment have been explored in term of waterbody, settlements, barren land, crop land, spare vegetation, and dense vegetation for the selected years. Furthermore, accuracy assessment and Kappa coefficient have been

investigated to evaluate the quality of information derived from the classified images. The results reveal that built-up land has increased by 25% because of development of Multan District during the last three decades. The area under dense vegetation has been decreased by 30% during the last three decades because of change in barren and built-up land. The settlements, barren and crop lands have increased to 25.2, 10.1, and 4.6%, respectively from 1990 to 2020. The values of kappa coefficient (0.84–0.85) showed very good level of classification. In addition, total volume of water loss in Multan District due to LULC change during the last three decades was 788 m^3. This volume of water is not reaching equitably to the farming community because of the LU and LC changes and urban settlements. The results indicated that remotely sensed image interpretation technique may be useful for reallocation of water among farmers in an equitable and efficient way. Furthermore, the findings of this study demonstrated that NDVI and unsupervised classification can be used to characterize and comprehend LULC changes in transitional areas such as in Multan, Pakistan.

Declarations

Conflict of interest The authors declare no competing interests.

References

Abdulkareem, J. H., Pradhan, B., Sulaiman, W. N. A., & Jamil, N. R. (2019). Prediction of spatial soil loss impacted by long-term land-use/land-cover change in a tropical watershed. *Geoscience Frontiers, 10*, 389–403. https://doi.org/10.1016/j.gsf.2017.10.010

Adnan, M. S. G., Abdullah, A. Y. M., Dewan, A., & Hall, J. W. (2020). The effects of changing land use and flood hazard on poverty in coastal Bangladesh. *Land Use Policy, 99*, 104868. https://doi.org/10.1016/j.landusepol.2020.104868

Ahmad, F. (2013). Land degradation pattern using geo-information technology for Kot Addu, Punjab Province, Pakistan. *Global Journal of Human-Social Science: B Geography Geo-Sciences, Disaster Environment, 13,* 1–16.

Ahmad, W., Jupp, L. B., & Nunez, M. (1992). Land cover mapping in a rugged terrain area using landsat mss data. *International Journal of Remote Sensing, 13,* 673–683. https://doi.org/10.1080/01431169208904145

Ahsen, R., Khan, Z. M., Farid, H. U., Shakoor, A., & Ali, I. (2020). Estimation of cropped area and irrigation water requirement using remote sensing and GIS. *JAPS: Journal of Animal & Plant Sciences*, *30*, 876–884. https://doi.org/10.36899/JAPS.2020.4.01030

Algorithms, M. O., Saeidian, B., Mesgari, M. S., & Pradhan, B. (2007). Irrigation water allocation at farm level based on temporal cultivation-related data using.

Allawai, M. F., & Ahmed, B. A. (2020). Using remote sensing and GIS in measuring vegetation cover change from satellite imagery in Mosul City, North of Iraq. *IOP Conference Series: Materials Science and Engineering, 757.* https://doi.org/10.1088/1757-899X/757/1/012062

Anchan, S. S., Shetty, A., Bhat, H. G., Chadaga, M. (2018). Land use and land cover change detection through spatial approach: A case study of Mangaluru Taluk, Karnataka. Journal of Geomatics *12*, 167–73

Anwar Khalid, K. (2019). Using unsupervised classification to determined land cover northren of Ninvah provianec by using Remote sensing Techniques. *Journal of Physics Conference Series*, *1294*. https://doi.org/10.1088/1742-6596/1294/9/092037

Araya, Y. H., & Hergarten, C. (2008). A comparison of pixel and object-based land cover classification: A case study of the Asmara region, Eritrea. *WIT Transactions on The Built Environment, 100,* 233–243. https://doi.org/10.2495/GEO080231

Brovkin, V., Boysen, L., Arora, V. K., Boisier, J. P., Cadule, P., Chini, L., et al. (2013). Effect of anthropogenic land-use and land-cover changes on climate and land carbon storage in CMIP5 projections for the twenty-first century. *Journal of Climate, 26,* 6859–6881. https://doi.org/10.1175/JCLI-D-12-00623.1

Butt, A., Shabbir, R., Ahmad, S. S., & Aziz, N. (2015). Land use change mapping and analysis using remote sensing and GIS: A case study of Simly watershed, Islamabad, Pakistan. *The Egyptian Journal of Remote Sensing and Space Science, 18,* 251–259. https://doi.org/10.1016/j.ejrs.2015.07.003

Chemura, A., Rwasoka, D., Mutanga, O., Dube, T., & Mushore, T. (2020). The impact of land-use/land cover changes on water balance of the heterogeneous Buzi sub-catchment, Zimbabwe. *Remote Sensing Applications: Society and Environment, 18,* 100292. https://doi.org/10.1016/j.rsase.2020.100292

Chen, X., Vierling, L., & Deering, D. (2005). A simple and effective radiometric correction method to improve landscape change detection across sensors and across time. *Remote Sensing of Environment, 98,* 63–79. https://doi.org/10.1016/j.rse.2005.05.021

Chen, X., Yang, D., Chen, J., & Cao, X. (2015). An improved automated land cover updating approach by integrating with downscaled NDVI time series data. *Remote Sensing*

Letters, 6, 29–38. https://doi.org/10.1080/2150704X.2014.998793

Choudhary, K., Boori, M. S., & Voz, V. (2015). Land use/cover disturbance due to tourism in Jesenı ̓ ky Mountain , Czech Republic: A remote sensing and GIS based approach 17–26. https://doi.org/10.1016/j.ejrs.2014.12.002

Clerici, N., Paracchini, M. L., & Maes, J. (2014). Land-cover change dynamics and insights into ecosystem services in European stream riparian zones. *Ecohydrology & Hydrobiology, 14,* 107–120. https://doi.org/10.1016/j.ecohyd.2014.01.002

Comission, E. (2018). Competence Centre on Foresight, Urbanisation worldwide [WWW Document]. URL https://knowledge4policy.ec.europa.eu/foresight/about_en (accessed 28 Nov 2021)

DeFries, R., Hansen, M., & Townshend, J. (1995). Global discrimination of land cover types from metrics derived from AVHRR pathfinder data. *Remote Sensing of Environment, 54,* 209–222. https://doi.org/10.1016/0034-4257(95)00142-5

Dewan, A., Kiselev, G., Botje, D., Mahmud, G. I., Bhuian, M. H., & Hassan, Q. K. (2021). Surface urban heat island intensity in five major cities of Bangladesh: Patterns, drivers and trends. *Sustainable Cities and Society, 71*, 102926. https://doi.org/10.1016/j.scs.2021.102926

Dewan, A. M., & Yamaguchi, Y. (2009). Land use and land cover change in Greater Dhaka, Bangladesh: Using remote sensing to promote sustainable urbanization. *Applied Geography, 29*, 390–401. https://doi.org/10.1016/j.apgeog.2008.12.005

Fahad, S., Wajid, N. (2020). Evaluating the climate change impact on water use efficiency of cotton-wheat in semiarid conditions using DSSAT model. J Water Climate Change, 11(4), pp.1661-1675. https://doi.org/10.2166/wcc.2019.179/622035/jwc2019179

Ganasri, B. P., & Dwarakish, G. S. (2015). Study of land use/land cover dynamics through classification algorithms for Harangi Catchment Area, Karnataka State, India. *Aquatic Procedia, 4,* 1413–1420. https://doi.org/10.1016/j.aqpro.2015.02.183

Goldblatt, R., Stuhlmacher, M. F., Tellman, B., Clinton, N., Hanson, G., Georgescu, M., et al. (2018). Using Landsat and nighttime lights for supervised pixel-based image classification of urban land cover. *Remote Sensing of Environment, 205,* 253–275. https://doi.org/10.1016/j.rse.2017.11.026

Gul, F., Ahmed, I., Ashfaq, M., Jan, D., Fahad, S., Li, X., Wang, D., Fahad, M., Fayyaz, M., & Shah, S. A. (2020). Use of crop growth model to simulate the impact of climate change on yield of various wheat cultivars under different agro-environmental conditions in Khyber Pakhtunkhwa , Pakistan.

Hassan, Z., Shabbir, R., Ahmad, S. S., Malik, A. H., Aziz, N., & Butt, A. (2016). Dynamics of land use and land cover change (LULCC) using geospatial techniques : A case study of Islamabad Pakistan. *Springerplus.* https://doi.org/10.1186/s40064-016-2414-z

Hayat, H., Akbar, T.A., Tahir, A.A., Hassan, Q.K., Dewan, A. and Irshad, M., (2019). Simulating current and future river-flows in the Karakoram and Himalayan regions of

Pakistan using snowmelt-runoff model and RCP scenarios. *Water, 11*(4) p.761. https://doi.org/10.3390/w11040761

Hussain, S., Mubeen, M., Akram, W., Ahmad, A., Habib-ur-Rahman, M., Ghaffar, A., Amin, A., Awais, M., Farid, H. U., Farooq, A., & Nasim, W. (2020). Study of land cover/land use changes using RS and GIS: a case study of Multan district, Pakistan. *Environmental Monitoring and Assessment, 192*. https://doi.org/10.1007/s10661-019-7959-1

Iqra, M., Amna, B., Shakeel, I., Fatima, K., Sehrish, L., Hamza, A., Fahad, S. (2020). Carbon Cycle in Response to Global Warming. in: Fahad, S., Hasanuzzaman, M., Alam, M., Ullah, H., Saeed, M., Khan, A.K., Adnan, M. (2020.),Environment, Climate, Plant and Vegetation Growth. Springer Publ Ltd, Springer Nature Switzerland AG. Part of Springer Nature. PP. 1-16. https://doi.org/10.1007/978-3-030-49732-3_1

Islam, K., Jashimuddin, M., Nath, B., & Kumar, T. (2018). The Egyptian Journal of Remote Sensing and Space Sciences Land use classification and change detection by using multi-temporal remotely sensed imagery : The case of Chunati wildlife sanctuary. *The Egyptian Journal of Remote Sensing and Space Science, 21,* 37–47. https://doi.org/10.1016/j.ejrs.2016.12.005

Kalra, K., Kumar Goswami, A., & Gupta, R. (2013). A comparative study of supervised image classification algorithms for satellite images. *International Journal of Electrical, 1,* 2320–2084.

Khatami, R., Mountrakis, G., & Stehman, S. V. (2016). A meta-analysis of remote sensing research on supervised pixel-based land-cover image classification processes: General guidelines for practitioners and future research. *Remote Sensing of Environment, 177,* 89–100. https://doi.org/10.1016/j.rse.2016.02.028

Li, M., Xu, Y., Fu, Q., Singh, V. P., Liu, D., & Li, T. (2020). Efficient irrigation water allocation and its impact on agricultural sustainability and water scarcity under uncertainty. *Journal of Hydrology, 586.* https://doi.org/10.1016/j.jhydrol.2020.124888

Liang, C., Zhang, R. C., Zeng, J., & Shen, Z. J. (2021). A land-use decision approach integrating thermal regulation, stormwater management, and economic benefits based on urbanization stage identification. *Science of the Total Environment, 779,* 146415. https://doi.org/10.1016/j.scitotenv.2021.146415

Lu, D., Mausel, P., Brondízio, E., & Moran, E. (2004). Change detection techniques. *International Journal of Remote Sensing, 25,* 2365–2401. https://doi.org/10.1080/0143116031000139863

Lu, D., & Weng, Q. (2007). A survey of image classification methods and techniques for improving classification performance. *International Journal of Remote Sensing, 28,* 823–870. https://doi.org/10.1080/01431160600746456

Mashwani Z.R. (2020). Environment, climate change and biodiversity. Environment, climate, plant and vegetation growth. Springer Publ Ltd, Springer Nature Switzerland AG. Part of Springer Nature, pp.473-502. https://doi.org/10.1007/978-3-030-49732-3_19

Meneses-Tovar, C. L. (2011). NDVI as indicator of degradation. *Unasylva, 62,* 39–46.

Milad, M., Ho, S., Firuz, M., & Ash, H. (2015). Measuring land cover change in Seremban, Malaysia using NDVI index. *Procedia Environmental Sciences, 30,* 238–243. https://doi.org/10.1016/j.proenv.2015.10.043

Mohammed, E. A., Hani, Z. Y., & Kadhim, G. Q. (2018). Assessing land cover/use changes in Karbala city (Iraq) using GIS techniques and remote sensing data. *Journal of Physics Conference Series, 1032.* https://doi.org/10.1088/1742-6596/1032/1/012047

Monserud, R. A., & Leemans, R. (1992). Comparing global vegetation maps with the Kappa statistic. *Ecological Modelling, 62,* 275–293. https://doi.org/10.1016/0304-3800(92)90003-W

Mubeen, M., Ashfaq, A., Hafiz, M.H., Muhammad, A., Farid, U.H., Mazhar, S., Muhammad, S., Asad, A., Amjed, A., Fahad, S., Wajid, N. (2020). Evaluating the climate change impact on water use efficiency of cotton-wheat in semiarid conditions using DSSAT model. J Water Climate Change, 11(4), pp.1661-1675. https://doi.org/10.2166/wcc.2019.179/622035/jwc2019179

Nuñez, M. N., Ciapessoni, H. H., Rolla, A., Kalnay, E., & Cai, M. (2008). Impact of land use and precipitation changes on surface temperature trends in Argentina. *Journal of Geophysical Research: Atmospheres, 113,* 1–11. https://doi.org/10.1029/2007JD008638

Pal, S., & Ziaul, S. (2017). The Egyptian Journal of Remote Sensing and Space Sciences Detection of land use and land cover change and land surface temperature in English Bazar urban centre. *The Egyptian Journal of Remote Sensing and Space Science, 20,* 125–145. https://doi.org/10.1016/j.ejrs.2016.11.003

Patela, N. N., Angiuli, E., Gamba, P., Gaughan, A., Lisini, G., Stevens, F. R., Tatem, A. J., & Trianni, G. (2015). Multitemporal settlement and population mapping from landsatusing google earth engine. *International Journal of Applied Earth Observation and Geoinformation, 35,* 199–208. https://doi.org/10.1016/j.jag.2014.09.005

Quyen, N. T. N., Liem, N. D., & Loi, N. K. (2014). Effect of land use change on water discharge in Srepok watershed, Central Highland, Viet Nam. *International Soil and Water Conservation Research, 2,* 74–86. https://doi.org/10.1016/S2095-6339(15)30025-3

Rahman, M.H., Ahmad, A., Wajid, A., Hussain, M., Rasul, F., Ishaque, W., Islam, M.A., Shelia, V., Awais, M., Ullah, A. and Wahid, A., (2019). Application of CSM-CROPGRO-Cotton model for cultivars and optimum planting dates: Evaluation in changing semi-arid climate. Field Crops Research, 238, pp.139-152. http://dx.doi.org/10.1016/j.fcr.2017.07.007

Rahman, A., Kumar, S., Fazal, S., & Siddiqui, M. A. (2012). Assessment of land use/land cover change in the North-West District of Delhi using remote sensing and GIS techniques. *Journal of the Indian Society of Remote Sensing, 40,* 689–697. https://doi.org/10.1007/s12524-011-0165-4

Rahman, M., Ningsheng, C., Mahmud, G. I., Islam, M. M., Pourghasemi, H. R., Ahmad, H., Habumugisha, J. M., Washakh, R. M. A., Alam, M., Liu, E., Han, Z., Ni, H., Shufeng, T., & Dewan, A. (2021). Flooding and its relationship with land cover change, population growth, and road density. *Geoscience Frontiers, 12,* 101224. https://doi.org/10.1016/j.gsf.2021.101224

Ranagalage, M., Morimoto, T., & Simwanda, M. (2021). Spatial analysis of urbanization patterns in four rapidly growing South Asian cities using Sentinel-2 Data 1–25.

Rawat, J. S. (2015). Monitoring land use / cover change using remote sensing and GIS techniques: A case study of Hawalbagh block, district Almora, Uttarakhand, India. *The Egyptian Journal of Remote Sensing and Space Science, 18,* 77–84. https://doi.org/10.1016/j.ejrs.2015.02.002

Rawat, J. S., Biswas, V., & Kumar, M. (2013). Changes in land use/cover using geospatial techniques: A case study of Ramnagar town area, district Nainital, Uttarakhand, India. *The Egyptian Journal of Remote Sensing and Space Science, 16,* 111–117. https://doi.org/10.1016/j.ejrs.2013.04.002

Roy, P., Chandra Pal, S., Chakrabortty, R., Chowdhuri, I., Malik, S., & Das, B. (2020). Threats of climate and land use change on future flood susceptibility. *Journal of Cleaner Production, 272*, 122757. https://doi.org/10.1016/j.jclepro.2020.122757

Rujoiu-Mare, M. -R., & Mihai, B. -A. (2016). Mapping land cover using remote sensing data and GIS techniques: A case study of Prahova Subcarpathians. *Procedia Environmental Sciences, 32*, 244–255. https://doi.org/10.1016/j.proenv.2016.03.029

Sahebjalal, E., & Dashtekian, K. (2013). Analysis of land use-land covers changes using normalized difference vegetation index (NDVI) differencing and classification methods. *African Journal of Agricultural Research, 8*, 4614–4622. https://doi.org/10.5897/AJAR11.1825

Setiawan, Y., Rustiadi, E., Yoshino, K., Liyantono, E., & Effendi, H. (2014). Assessing the seasonal dynamics of the Java's paddy field using MODIS Satellite Images. *ISPRS International Journal of Geo-Information, 3*, 110–129. https://doi.org/10.3390/ijgi3010110

Taluk, M. (2018). Land Use and Land Cover Change Detection through Spatial Approach: A Case Study of, *12*, 167–173.

Tian, F., Fensholt, R., Verbesselt, J., Grogan, K., Horion, S., & Wang, Y. (2015). Evaluating temporal consistency of long-term global NDVI datasets for trend analysis. *Remote Sensing of Environment, 163,* 326–340. https://doi.org/10.1016/j.rse.2015.03.031

Udin, W. S., & Zahuri, Z. N. (2017). Land use and land cover detection by different classification systems using remotely sensed data of Kuala Tiga, Tanah Merah Kelantan, Malaysia. *Journal Tropology Resource Sustainable Science, 5,* 145–151.

Ullah, S., Tahir, A. A., Akbar, T. A., Hassan, Q. K., Dewan, A., Khan, A. J., & Khan, M. (2019). Remote sensing-based quantification of the relationships between land use land cover changes and surface temperature over the lower Himalayan region. *Sustain*, 11. https://doi.org/10.3390/su11195492

Vicente-Serrano, S. M., Camarero, J. J., Olano, J. M., Martín-Hernández, N., Peña-Gallardo, M., Tomás-Burguera, M., et al. (2016). Diverse relationships between forest growth and the Normalized Difference Vegetation Index at a global scale. *Remote Sensing of Environment, 187,* 14–29. https://doi.org/10.1016/j.rse.2016.10.001

Wahyunto, W., Supriatna, W., & Agus, F. (2013). Land use change and recommendation for sustainable development of peatland for agriculture: Case study at Kubu Raya and Pontianak Districts, West Kalimantan. Indones. *Journal of Agricultural Science*, *11*, 32. https://doi.org/10.21082/ijas.v11n1.2010.p32-40

Wang, Q., Riemann, D., Vogt, S., & Glaser, R. (2014). Impacts of land cover changes on climate trends in Jiangxi province China. *International Journal of Biometeorology, 58*, 645–660. https://doi.org/10.1007/s00484-013-0645-z

Xiuwan, C. (2002). Using remote sensing and GIS to analyse land cover change and its impacts on regional sustainable development. *International Journal of Remote Sensing, 23*, 107–124. https://doi.org/10.1080/01431160010007051

Yohannes, H., Soromessa, T., Argaw, M., & Dewan, A. (2021). Impact of landscape pattern changes on hydrological ecosystem services in the Beressa watershed of the Blue Nile Basin in Ethiopia. *Science of the Total Environment, 793*, 148559. https://doi.org/10.1016/j.scitotenv.2021.148559

Zaidi, S. M., Akbari, A., Samah, A. A., & Kong, N. S. (2017). Landsat-5 time series analysis for land use/land cover change detection using NDVI and semi-supervised classification techniques. *Polish Journal of Environmental Studies*, *26*, 2833–2840. https://doi.org/10.15244/pjoes/68878

Zhao, Y., Ma, S., Fan, J., & Cai, Y. (2021). Examining the effects of land use on carbon emissions: Evidence from Pearl River Delta.

Zhou, X., & Chen, H. (2018). Impact of urbanization-related land use land cover changes and urban morphology changes on the urban heat island phenomenon. *Science of the Total Environment, 635*, 1467–1476. https://doi.org/10.1016/j.scitotenv.2018.04.091